RSC Advances

PAPER

View Article Online
View Journal | View Issue



Cite this: *RSC Adv.*, 2025, **15**, 25441

# Pigments with antimicrobial and cytotoxic activities from the coprophilous fungus *Fusarium solani* isolated from horse dung†

Bel Youssouf G. Mountessou,[a] Iliassou L. Mouafon,[b] Rukesh Maharjan,[c] Joseph Tchamgoue,[d] Gesquiere Laure M. Tiani,[e] Patrick Dibouloul,[a] Muhammad I. Choudhary[c] and Simeon F. Kouam*[a]

Four previously undescribed phenazine-derived pigments (**1–4**), along with seventeen known compounds, were isolated from a *Fusarium solani* strain cultured on solid rice medium. Structural elucidation of the new compounds was achieved through extensive spectroscopic analysis, while known compounds were identified by comparison with literature data. The antimicrobial and cytotoxic activities of the isolated compounds were assessed. Compounds **2**, **5**, and **11** exhibited weak antifungal activity against *Candida albicans* at 200 μM, while compounds **5**, **6**, **11**, **12**, **15**, and **20** demonstrated moderate antibacterial effects against *Staphylococcus aureus* at the same concentration. Notably, compound **4** showed significant cytotoxicity against breast cancer cells (MCF-7, $IC_{50}$ = 6.8 μM), and moderate cytotoxicity against cervical cancer cells (HeLa, $IC_{50}$ = 25.0 μM). Moreover, the known quinone-derived pigments **10**, **12**, and **13** displayed potent cytotoxic activities against the three tested cancer cell lines (MCF-7, PC3, and HeLa). These results highlight the potential of these compounds as promising bioactive agents for cancer treatment.

Received 12th June 2025
Accepted 9th July 2025

DOI: 10.1039/d5ra04180e

rsc.li/rsc-advances



## 1. Introduction

Coprophilous fungi, which thrive in the dung of herbivores or decaying organic matter, play a crucial ecological role in nutrient cycling and have emerged as promising sources of bioactive metabolites.[1–5] Among these fungi, *Fusarium solani* is a ubiquitous species with both pathogenic and biotechnological significance. While primarily studied for its role in plant diseases,[6] *F. solani* also produces a diverse range of secondary metabolites, including water-soluble pigments such as phenazines, quinones, and furans, as well as alkaloids, terpenoids, and polyketides.[7,8] These compounds exhibit a broad spectrum of bioactivities—ranging from antimicrobial and anticancer to antioxidant and immunomodulatory effects—making them attractive candidates for pharmaceutical and industrial applications.[7–9] Despite their potential, only a limited number of these fungal pigments have been thoroughly investigated for their biological properties.[7]

Given the ecological adaptability of *F. solani*[10,11] and its underexplored chemical diversity, we sought to characterise its metabolic potential as part of our ongoing search for bioactive fungal natural products.[12–14] In this study, a strain of *F. solani* was isolated from horse dung, leading to the identification of four new fungal metabolites (**1–4**, Fig. 1) alongside seventeen known derivatives (**5–21**) (Fig. S1†). Structural elucidation was conducted using spectroscopic techniques, and the antimicrobial and cytotoxic activities of the compounds were assessed. Our findings not only expand the known chemical repertoire of *F. solani* but also provide insights into the therapeutic potential of fungal pigments, paving the way for future drug discovery efforts.

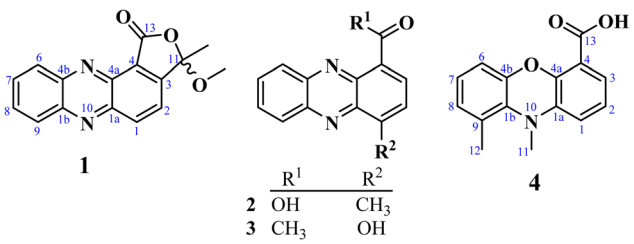


Fig. 1 Chemical structures of compounds **1–4**.

[a]*Department of Chemistry, Higher Teacher Training College, University of Yaoundé I, P. O. Box 47, Yaoundé, Cameroon. E-mail: kfogue@yahoo.com*

[b]*Department of Pharmaceutical Sciences, Tshwane University of Technology, P. O. Box 0083, Pretoria, South Africa*

[c]*H.E.J. Research Institute of Chemistry, International Centre for Chemical and Biological Sciences (ICCBS), University of Karachi, Karachi-75270, Pakistan*

[d]*Department of Organic Chemistry, Faculty of Science, University of Yaoundé I, P. O. Box 812, Yaoundé, Cameroon*

[e]*Division of Wood Chemistry, University Institute of Wood Technology Mbalmayo, P. O. Box 306, Mbalmayo, Cameroon*

† Electronic supplementary information (ESI) available. See DOI: https://doi.org/10.1039/d5ra04180e

## 2. Results and discussion

### 2.1. Structural elucidation of compounds

Well-grown *Fusarium solani* cultures on Yeast-Mold-Agar (YMA) plates were fermented in solid rice medium and extracted with ethyl acetate, yielding 4.2 g of organic extract. The extract was subjected to repeated silica gel and Sephadex LH-20 column chromatography, which resulted in several fractions. These fractions were further purified by normal- and reversed-phase preparative HPLC, leading to the isolation of twenty-one compounds, of which compounds **1–4** were hitherto unknown.

Fusaphenazinone (**1**) was obtained as a yellowish pigment. Its molecular formula, $C_{16}H_{12}N_2O_3$, was determined by high-resolution electron ionization mass spectrometry (HREIMS), which revealed the molecular ion peak $[M]^{\cdot+}$ (Fig. S2†) at *m*/*z* 280.0846 (calcd for 280.0848), corresponding to twelve double bond equivalents (DBE). The IR spectrum showed strong absorption bands for a conjugated lactone carbonyl, C–O, and C–H stretching vibrations at 1769, 1188, and 2923–2852 $cm^{-1}$, respectively (Fig. S3†). The UV spectrum (Fig. S4†) exhibited absorption maxima at $\lambda_{max}$ 256, 267, and 371 nm characteristic of phenazine derivatives[15] and related compounds.[16] Analysis of the NMR (Table 1) and HSQC data (Fig. S8†) revealed the presence of a methyl group ($\delta_{H/C}$ 1.95/24.7), a methoxy group ($\delta_{H/C}$ 3.17/51.6), six aromatic methines ($\delta_{H/C}$ 8.60/138.4, 8.50/130.7, 8.28/129.9, 7.94/132.2, 7.94/131.9, 7.87/122.5), and seven quaternary carbons ($\delta_C$ 165.3, 154.7, 144.5, 144.0, 139.0, 123.0, 106.0) (Fig. S5–S7†). The $^{13}C$ chemical shifts observed in the range $\delta_C$ 144.0–139.0 further confirmed the phenazine core structure in compound **1** (Fig. 1). This structure was identified as a 1,2-disubstituted scaffold, as the $^1H$ NMR spectrum (Fig. S5†) revealed two sets of proton signals: (a) two sharp doublets of *ortho*-coupled protons at $\delta_H$ 8.60 and 7.87 (1H each, d, 8.5 Hz, H-2, H-1), and (b) a pair of doublets of doublets at $\delta_H$ 8.50 and 8.28 (1H each, dd, 2.0; 8.5 Hz, H-9, H-6), along with a signal for two overlapping protons at $\delta_H$ 7.95 (H-7 and H-8). The 1-proton sharp doublet at $\delta_H$ 7.87 showed HMBC cross-peaks with carbon resonances at $\delta_C$ 143.6 (C-1a), 123.0 (C-4), and the hemiketal carbon signal at $\delta_C$ 106.7 (C-11). These key HMBC correlations helped establish the attachment of the hemiketal carbon at C-3 of the phenazine skeleton, to an acid-derived carbonyl group at C-4. Consistent with the molecular weight of 280 and the thirteen degrees of unsaturation, the acid-derived carbonyl group was cyclized with the hydroxyl of the hemiketal group to form a lactone. Additional HMBC correlations were observed between the hemiketal carbon signal ($\delta_C$ 106.7) and the proton signals of both the methyl ($\delta_H$ 1.95) and the methoxy ($\delta_H$ 3.17) groups (Fig. S9†). These findings were further supported by COSY correlations (Fig. 2 and S10†) and by electron ionization mass spectrometry (EI-MS), which showed important ion peaks at *m*/*z* 265 $[M-15]^{\cdot+}$, *m*/*z* 249 $[M-31]^{\cdot+}$, and *m*/*z* 178 $[C_{12}H_6N_2]^{\cdot+}$ (Fig. S2†). The proposed structure of compound **1** was fully confirmed by HMBC, DEPT, and COSY spectra. Fig. 2 illustrates key HMBC and COSY correlations of compound **1**. However, the absence of optical rotation indicates that compound **1** exists as a racemic mixture at C-11. While chiral HPLC analysis could have enabled the separation of the enantiomers and definitive determination of their absolute

Table 1 $^1H$ and $^{13}C$ NMR data of compounds **1–4**

| | **1**[a] | | **2**[b] | | **3**[c] | | **4**[b] | |
|---|---|---|---|---|---|---|---|---|
| No. | $\delta_H$ mult. (*J* in Hz) | $\delta_C$, type | $\delta_H$ mult. (*J* in Hz) | $\delta_C$, type | $\delta_H$ mult. (*J* in Hz) | [d]$\delta_C$, type | $\delta_H$ mult. (*J* in Hz) | [d]$\delta_C$, type |
| 1 | 8.60 d (8.5) | 138.4 (CH) | — | 142.9 (C) | — | 157.1 (C) | 8.52 dd (1.6; 8.8) | 135.0 (CH) |
| 1a | — | 143.6 (C) | — | 145.0 (C) | — | 142.2 (C) | — | 143.1 (C) |
| 1b | — | 144.0 (C) | — | 143.1 (C) | — | 144.7 (C) | — | 139.7 (C) |
| 2 | 7.87 d (8.5) | 122.5 (CH) | 7.85 d (7.2) | 129.5 (CH) | 8.13 d (8.8) | 128.3 (CH) | 8.03 dd (6.4; 8.8) | 130.4 (CH) |
| 3 | — | 154.6 (C) | 8.86 d (7.2) | 137.5 (CH) | 8.23 d (8.8) | 130.9 (CH) | 8.97 dd (1.6; 6.4) | 137.3 (CH) |
| 4 | — | 123.0 (C) | — | 122.7 (C) | — | 133.9 (C) | — | 125.0 (C) |
| 4a | — | 139.0 (C) | — | 140.3 (C) | — | 144.8 (C) | — | 139.0 (C) |
| 4b | — | 144.5 (C) | — | 139.4 (C) | — | 145.3 (C) | — | 144.5 (C) |
| 6 | 8.50 dd (2.0; 8.5) | 130.7 (CH) | 8.26 d (8.8) | 127.8 (CH) | 8.33 d (8.8) | 131.4 (CH) | 8.18 d (8.8) | 128.2 (CH) |
| 7 | 7.95 m | 132.2 (CH) | 7.99 ddd (8.8; 6.4; 1.6) | 133.0 (CH) | 7.91 pseudo t (8.0) | 132.0 (CH) | 7.87 dd (7.2; 8.8) | 131.9 (CH) |
| 8 | 7.95 m | 131.9 (CH) | 7.95 ddd (8.8; 6.4; 1.6) | 131.2 (CH) | 7.96 pseudo t (8.0) | 133.3 (CH) | 7.83 d (7.2) | 132.6 (CH) |
| 9 | 8.28 dd (2.0; 8.5) | 129.9 (CH) | 8.37 d (8.8) | 130.4 (CH) | 8.21 d (8.8) | 129.9 (CH) | — | 135.8 (C) |
| 11 | — | 106.7 (C) | — | — | — | — | 3.47 *s* | 50.8 ($CH_3$) |
| 12 | — | — | — | — | — | — | 2.94 s | 18.4 ($CH_3$) |
| 13 | — | 165.3 (C) | — | 166.4 (C) | — | 201.3 (C) | — | 166.1 (C) |
| 11-$CH_3$ | 1.95 | 24.7 ($CH_3$) | — | — | — | — | — | — |
| 11-$OCH_3$ | 3.17 | 51.6 ($CH_3$) | — | — | — | — | — | — |
| 1-$CH_3$ | — | — | 3.01 s | 18.3 ($CH_3$) | — | — | — | — |
| 13-$CH_3$ | — | — | — | — | 2.85 *s* | 30.8 ($CH_3$) | — | — |
| 13-OH | — | — | 15.65 *s* | — | — | — | 15.81 *s* | — |

[a] Data were recorded in $CDCl_3$ at 500 MHz for $^1H$ NMR and 150 MHz for $^{13}C$ NMR. [b] Data were recorded in $CDCl_3$ at 800 MHz for $^1H$ NMR and 200 MHz for $^{13}C$ NMR. [c] Data were recorded in $CD_3OD$ at 500 MHz for $^1H$ NMR and 125 MHz for $^{13}C$ NMR. [d] Chemical shifts for $^{13}C$ were retrieved from the HSQC-DEPT spectra, as the $^{13}C$ NMR spectra were not recorded.

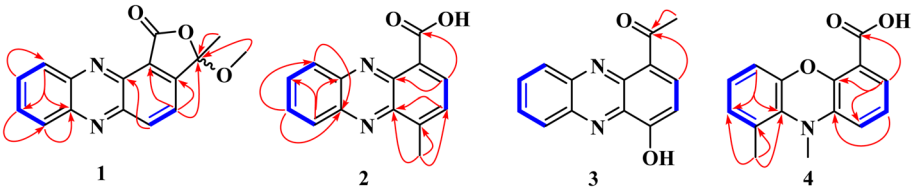


Fig. 2 Key COSY (▬) and HMBC (↷) correlations of compounds **1**–**4**.

configurations, this approach was precluded by the unavailability of an appropriate chiral column and the insufficient amount of material (1.3 mg).

4-Methylphenazine-1-carboxylic acid (**2**) was obtained as a yellowish, gummy pigment. The molecular formula $C_{14}H_{10}N_2O_2$ was assigned to the compound based on HREI-MS data (*m*/*z* 238.0744; calcd for 238.0742) (Fig. S11†), corresponding to 11° of unsaturation. The broadband decoupled $^{13}C$ NMR spectrum of **2** (Fig. S15†) showed 14 carbon signals, which were sorted by DEPT and HSQC techniques into four methyl, six methine, and seven quaternary carbons, including a carbonyl signal ($\delta_C$ 166.4) associated with the acid group, and four nitrogenized carbons from phenazine moiety ($\delta_C$ 145.0, 143.1, 140.3, 139.4). The IR spectrum of **2** (Fig. S12†) displayed characteristic vibration bands due to a methyl group (2922–2852 $cm^{-1}$ and 760–741 $cm^{-1}$), a conjugated acid carbonyl group (1715 $cm^{-1}$), and benzene rings (1569–1532 $cm^{-1}$). The UV-vis spectrum of **2** (Fig. S13†) showed absorption maxima at $\lambda_{max}$ 257, 266, and 372 nm, similar to those of phenazine derivatives, as observed in compound **1**. In the $^1H$ NMR spectrum of **2** (Fig. S14†), the deshielded singlet signal at $\delta_H$ 15.65 in the downfield region indicated the presence of a carboxylic acid group, with its OH group chelated to the nitrogen of the phenazine moiety. Similar to **1**, the $^1H$ NMR spectrum of **2** displayed a pair of doublets at $\delta_H$ 8.86 and 7.85 (1H each, d, 7.2 Hz, H-3, H-2), assignable to two *ortho*-coupled protons, along with another pair of doublets at $\delta_H$ 8.26 and 8.37 (1H each, d, 8.8 Hz, H-6, H-9), and proton signals at $\delta_H$ 7.99 and 7.95 (1H each, ddd, 8.8; 6.4; 1.6 Hz, H-7, H-8) (Table 1). HMBC cross-peaks observed between the 3-proton signal at $\delta_H$ 3.01 (3H, *s*) and the carbon signals at $\delta_C$ 145.0 (C-1a), 142.9 (C-1), and 129.5 (C-2) permitted to attach the methyl group at C-1 of the phenazine moiety. Additional HMBC correlations supporting the structure of **2** include the correlation between the proton signal at $\delta_H$ 8.86 (H-3) and the carbon signals at $\delta_C$ 166.4 (COOH), 145.0 (C-1a), and 140.3 (C-4a) (Fig. 2). The structure of **2** was further confirmed by DEPT, HSQC, and COSY spectra (Fig. S16–S19†), and its spectroscopic data were consistent with those of 4-methylphenazine-1-carboxylic acid, a synthetic compound.[17] To the best of our knowledge, this is the first report of its spectroscopic data as a naturally occurring secondary metabolite.

1-Acetyl-4-hydroxyphenazine (**3**) was obtained as a gummy, yellow pigment. Its molecular formula, $C_{14}H_{10}N_2O_2$, with 11 double bond equivalents, was determined from HREI-MS (Fig. S20†), which showed the molecular weight at *m*/*z* 238.0740, matching the calculated value of 238.0742. The IR spectrum exhibited strong absorption bands for hydroxyl (3400 $cm^{-1}$) and conjugated carbonyl (1590 $cm^{-1}$) groups, along with characteristic absorption bands for aliphatic C–H stretching vibrations at 2919 and 2851 $cm^{-1}$ (Fig. S21†). Similar to compounds **1** and **2**, the UV spectrum of compound **3** displayed absorption maxima characteristic of phenazines at $\lambda_{max}$ 247, 264, and 368 nm (Fig. S22†). The $^1H$ NMR spectrum of **3**, recorded in $CD_3OD$ (Fig. S23†), displayed similarities to the spectra of compounds **1** and **2**, with more distinct multiplicities for the aromatic protons. The structural elucidation of **3** was straightforward, as it was inferred from the structures of **1** and **2**. In the $^1H$ NMR spectrum of **3**, two sets of proton signals on the phenazine core were observed: (a) a pair of doublets for *ortho*-coupled protons at $\delta_H$ 8.33 and 8.21 (1H each, d, 8.8 Hz, H-12, H-9), each coupling with a pair of pseudo-triplets at $\delta_H$ 7.96 and 7.91 (1H each, pseudo *t*, 8.0 Hz, H-10, H-11), and (b) a pair of doublets at $\delta_H$ 8.23 and 8.13 (1H each, d, 8.8 Hz, H-2, H-3) (Table 1 and Fig. S23†). HMBC cross-peaks between the 1-proton doublet at $\delta_H$ 8.23 and the carbon signals at $\delta_C$ 201.3 and 144.8 confirmed the presence of a phenazine moiety in **3**, with an acetyl group at position C-1. This acetyl group was further confirmed by HMBC cross-peaks between the 3-proton singlet at $\delta_H$ 2.85 and the deshielded carbon signal at $\delta_C$ 201.3 (Fig. S25†). Additional HMBC correlations were observed between the proton signal at $\delta_H$ 8.13 and the carbon signals at $\delta_C$ 142.2 (C-5) and 133.9 (C-1), as well as between the proton signal at $\delta_H$ 7.96 and the carbon signals at $\delta_C$ 144.8 (C-8) and 131.4 (C-12). The structure of **3** was fully supported by other spectra, including HSQC (Fig. S24†) and COSY (Fig. S26†) spectra, with key HMBC and COSY correlations illustrated in Fig. 2.

Compound **4**, named 9,10-dimethylphenoxazine-4-carboxylic acid, was obtained as a yellowish pigment. Its molecular formula, $C_{15}H_{13}NO_3$, was established from HREI-MS (Fig. S27†), which showed the molecular ion peak $[M]^{\cdot+}$ at *m*/*z* 255.0893 (calcd for 255.0895). The IR spectrum revealed absorption bands for hydroxyl, methyl, and conjugated carbonyl groups at 3366, 2923–2853, and 1737 $cm^{-1}$, respectively (Fig. S28†), while absorption maxima at $\lambda_{max}$ 262, and 374 nm observed in the UV spectrum (Fig. S29†) were also suggestive of a phenazine derivative. The $^1H$ NMR spectrum of compound **4** (Fig. S30†) exhibited similarities to those of compounds **1**–**3**, with additional signals of two deshielded methyl groups at $\delta_H$ 3.47 and 2.94, along with a 1-proton singlet at $\delta_H$ 15.81, assigned to a chelated OH group of carboxylic acid. The spectrum also revealed six aromatic proton signals, sorted into two sets: (a) $\delta_H$ 8.97 (dd, 1.6; 6.4 Hz), 8.03 (dd, 6.4; 8.8 Hz), and 8.52 (dd, 1.6; 8.8 Hz), and (b) $\delta_H$ 8.18 (d, 8.8 Hz), 7.87 (dd,

7.2; 8.8 Hz), and 7.83 (d, 7.2 Hz), further supporting the phenazine derivative structure. However, the $^{13}$C NMR and DEPT spectra, recorded on an 800 MHz NMR CryoProbe, did not show any peaks due to the low sample amount (0.2 mg). Approximate $^{13}$C chemical shift values as listed in Table 1, were obtained from the HSQC and HMBC spectra (Fig. S31 and S32†). The structural elucidation of this compound was also facilitated by its similarities to compound **2**. In the HMBC spectrum, cross-peaks were observed between the proton signal at $\delta_H$ 8.97 and the carbon resonances at $\delta_C$ 166.1, 139.1, and 134.8, also between the proton signal at $\delta_H$ 8.52 and the carbon signal at $\delta_C$ 137.2. Further HMBC correlations were observed between the proton signal at $\delta_H$ 8.18 and the carbon signals at $\delta_C$ 139.5, and 132.6, and between the proton signal at $\delta_H$ 8.03 and the carbon signals at $\delta_C$ 143.1 and 125.0 (Fig. 2). Additionally, the methyl proton signals at $\delta_H$ 2.94 correlated with the carbon signals at $\delta_C$ 139.5, 135.8, and 132.6. The deshielded proton signal at $\delta_H$ 3.47 was found to be attached to the nitrogen atom. Consistent with the molecular mass and formula, another nitrogen atom in the phenazine core was replaced by an oxygen atom. The structure of compound **4** was also supported by the COSY spectrum (Fig. S33†), and all protons and carbons were assigned using HSQC cross-peaks. The structure was further validated by important ion fragments at *m/z* 210 $[M-45]^{\bullet+}$ (*i.e.*, M–COOH), *m/z* 180 $[M-75]^{\bullet+}$ (*i.e.*, M–COOH–2 × $CH_3$), *m/z* 120 $[C_6H_3–COOH]^{\bullet+}$, and *m/z* 90 $[C_6H_3–CH_3]^{\bullet+}$ (Fig. S2†).

The known compounds (Fig. S1†) were identified as phenazine-1-carboxylic acid (**5**),[18] phenazine-1-carboxamide (**6**),[15,19] lumichrome (**7**),[20] anhydrofusarubin (**8**),[21,22] 3-methyl ether-fusarubin (**9**),[21,23] fusarubin (**10**),[21,24,25] bostrycoidin (**11**),[26] javanicin (**12**),[21,24,27] 5,8-dihydroxy-2-methoxy-6-hydroxymethyl-7-(2-hydroxypropyl)-1,4-naphthalenedione (**13**),[28] 1,3,6-trihydroxy-7-(1-hydroxyethyl)anthracene-9,10-dione (**14**),[29,30] 2,3-dihydro-5-hydroxy-4-hydroxymethyl-8-methoxy-2-methylnaphtho[1,2-*b*]furan-6,9-dione (**15**),[31] 5,7-dimethoxyisobenzofuran-1(3*H*)-one (**16**),[32] apocynin (**17**),[33] 2-heptyl-3-hydroxy-4(1*H*)-quinolone (**18**),[34] haplacutine F (**19**),[35,36] ganodermaside D (**20**),[37] cerevisterol (**21**).[38,39]

It is worth noting that, although nitrogen-containing heterocyclic compounds such as phenazines are often associated with the secondary metabolism of certain bacteria and fungi, they have been reported to be produced by some *Fusarium* species.[7] However, to the best of our knowledge, no phenazine has been isolated and reported from *Fusarium*. Phenazine production in *Fusarium* is influenced by environmental factors like temperature, pH, oxygen availability, and the composition of the culture medium used during fermentation.[40,41]

## 2.2. Antimicrobial and cytotoxic activities

Water-soluble pigments, including phenazines, quinones, furans, flavins, pyrans, and others, are known in the food industry to exhibit antimicrobial, cytotoxic, and antioxidant activities.[7] Thus, the isolated compounds, sorted into phenazine-derived pigments (**1–4**), flavins (**7**), quinones (**8–15**), furanone (**16**), quinolones (**18** and **19**), the steroidal compounds **20** and **21**, and others were assessed for their antimicrobial and cytotoxic activities.

**2.2.1 Antimicrobial activities.** Selected isolated compounds were evaluated for their antimicrobial activities (Table 2). None of the compounds exhibited activity against Gram-negative *Escherichia coli* (ATCC 25922). However, six compounds (**5**, **6**, **11**, **12**, **15**, and **20**) demonstrated inhibitory effects against two *Staphylococcus aureus* strains, including methicillin-resistant MRSA (NCTC 13277) and a biofilm-forming strain (ATCC 6538). Compounds **6** and **12** showed weak activity against both *S. aureus* strains (MIC = 200 μM), while **5**, **11**, **15**, and **20** displayed strain-dependent activity, with higher MICs against NCTC 13277 (400 μM) than against ATCC 6538 (200 μM). These results are consistent with previously reported anti-staphylococcal activities for phenazine-1-carboxylic acid (**5**),[42] phenazine-1-carboxamide (**6**),[43] bostrycoidin (**11**),[26] javanicin (**12**),[21,44] and ganodermaside D (**20**).[45] Additionally, compound **15**, previously characterised for anti-inflammatory properties, now shows antibacterial activity against *S. aureus*. In antifungal assays, three compounds (**2**, **5**, and **11**) inhibited *Candida albicans* at 200 μM, further supporting their reported antifungal potential.[46–48]

Table 2 Results of antimicrobial and cytotoxic activities of selected isolated compounds[a]

| | Antimicrobial (MIC, μM) | | | | Cytotoxicity[b] ($IC_{50}$, μM) | | |
|---|---|---|---|---|---|---|---|
| Compounds | SA1 | SA2 | EC | CA | MCF-7 | PC3 | HeLa cell |
| **1** | — | — | nt | nt | nd | nt | nd |
| **2** | — | — | — | 200 | nd | nt | nd |
| **3** | — | — | — | — | ✗ | nt | nd |
| **4** | nt | nt | nt | nt | 6.8 | nd | 25.0 |
| **5** | 400 | 200 | — | 200 | nd | nt | 36.2 |
| **6** | 200 | 200 | — | — | 37.1 | 35.0 | 8.9 |
| **7** | — | — | nt | — | ✗ | nt | nt |
| **8** | — | — | — | nt | nd | 27.6 | 49.0 |
| **9** | — | — | — | — | nd | nt | nt |
| **10** | — | — | — | — | 9.7 | 8.6 | 9.8 |
| **11** | 400 | 200 | — | 200 | nd | 14.7 | ✗ |
| **12** | 200 | 200 | — | — | 7.2 | 7.3 | 8.3 |
| **13** | — | — | — | — | 9.4 | 7.3 | 7.1 |
| **14** | — | — | — | — | nt | nt | nt |
| **15** | 400 | 400 | — | — | 19.4 | 7.1 | 29.4 |
| **16** | — | — | — | — | nd | 17.9 | ✗ |
| **18** | — | — | — | — | 10.8 | 14.3 | nd |
| **19** | — | — | nt | — | ✗ | nt | ✗ |
| **20** | 400 | 200 | — | nt | 12.2 | 6.4 | 91.2 |
| **21** | — | — | — | — | ✗ | nd | nt |
| Ofloxacin[c] | 25 | 25 | 1–2 | ✗ | nt | nt | nt |
| Amphotericin[d] | ✗ | ✗ | ✗ | 0.4–1.0 | nt | nt | nt |
| Doxorubicin[e] | nt | nt | nt | nt | 0.10 | 0.50 | 0.36 |

[a] MIC = Minimum inhibitory concentration. [b] Tested in triplicate at each concentration, with $IC_{50}$ values representing mean ± SD from three independent experiments; — = inactive at MIC > 400 μM; nt = not tested; nd = not determined (as the dose-dependent inhibition curves did not reach 50% inhibition within the tested range of 6.25–100 μM); ✗ = inactive; SA1 = *Staphylococcus aureus* (NCTC 13277); SA2= *Staphylococcus aureus* biofilms (ATCC 6538); EC = *Escherichia coli* (ATCC 25922); CA = *Candida albicans* (ATCC 36082). [c] Standard antibacterial drug. [d] Standard antifungal drug. [e] Standard drug for cytotoxicity assay.

**2.2.2 Cytotoxic activities.** Selected isolated compounds (Table 2) were initially assessed at a concentration of 100 μM for their cytotoxic activities against breast (MCF-7), cervical (HeLa), and prostate (PC-3) cancer cell lines. The results showed that the new compound, 9,10-dimethylphenoxazine-4-carboxylic acid (**4**), exhibited potent cytotoxic activity against MCF-7 cell lines ($IC_{50}$ = 6.8 μM) and moderate activity against HeLa cell line ($IC_{50}$ = 25.0 μM). Compounds **1–3** were non-cytotoxic against MCF-7 and HeLa cells. Phenazine-1-carboxamide (**6**) showed potent cytotoxicity against HeLa cell line with $IC_{50}$ = 8.9 μM and moderate cytotoxic activity against MCF-7 and PC3 cell lines. Other pigments, including fusarubin (**10**), javanicin (**12**), and 5,8-dihydroxy-2-methoxy-6-hydroxymethyl-7-(2-hydroxypropyl)-1,4-naphthalenedione (**13**), displayed potent cytotoxic activity against all three cell lines. Anhydrofusarubin (**8**) exhibited moderate inhibition against PC3 and HeLa cancer cells. The potency of compound **8** was moderate against PC3 cancer cells ($IC_{50}$ = 27.6 μM) and inactive against MCF-7 breast cancer cells.

In contrast to the previous work of Trisuwan and collaborators (2010),[21] who reported moderate activity for compound **12** (javanicin) against MCF-7 breast cancer cells, our findings revealed a more potent cytotoxic profile, with an $IC_{50}$ value of 7.2 μM. To validate these results, we conducted additional dose–response experiments with compounds **10** and **12** across a concentration range of 6.25–100 μM. Compound **12** showed clear dose-dependent inhibition of MCF-7 cell growth, achieving 91.8% inhibition at 50 μM, 83.6% at 25 μM, 69.4% at 12.5 μM, and 45.2% at 6.25 μM (Fig. S34†). These differences in activity may stem from variations in experimental conditions or cell line characteristics. Further investigation using quantum structure–activity relationship (QSAR) analysis could help elucidate the molecular features underlying these divergent results. Additionally, ganodermaside D (**20**), a steroidal compound previously reported as an anti-aging agent by Weng and co-workers (2011),[37] exhibited moderate inhibitory activities against MCF-7 breast ($IC_{50}$ = 12.2 μM) and HeLa cervical ($IC_{50}$ = 91.2 μM) cancer cell lines. Its potency was good against PC3 prostate cancer cells ($IC_{50}$ = 6.4 μM).

**2.2.3 Mechanistic insights and future directions.** The current findings demonstrate that the anti-staphylococcal agents (**5**, **6**, **11**, **12**, **15**, **20**) and the antifungal compounds (**2**, **5**, **11**), exhibit moderate bioactivity against *S. aureus* and *C. albicans*, with MICs (200–400 μM). However, their inactivity against *E. coli* represents a major spectrum limitation. These results underscore the need for structural optimisation to enhance potency and broaden antimicrobial coverage. Rational medicinal chemistry approaches, such as bioisosteric replacement (*e.g.*, modifying phenazine derivatives **5** and **6** or quinones **11** and **12**), scaffold rigidification, and targeted functional group modifications, could transform these leads into more potent, broad-spectrum agents. The activity of compounds **5**, **6**, **11**, **12**, **15**, and **20** against resistant *S. aureus* strains (including MRSA), along with the antifungal effects of **2**, **5**, and **11** against *C. albicans*, provides a promising starting point for further development. The selective inhibition of Gram-positive bacteria over *E. coli* suggests outer membrane permeability barriers, while the antifungal mechanism may involve mitochondrial dysfunction or oxidative stress. Future optimisation strategies should explore hybrid scaffolds combining structural features of active anti-staphylococcal (**6**, **12**) and antifungal (**2**, **11**) compounds to improve Gram-negative activity while retaining efficacy against resistant Gram-positive and fungal pathogens.

In cytotoxicity assays, several compounds showed promising activity against breast (MCF-7), cervical (HeLa), and prostate (PC-3) cancer cell lines, with derivatives such as **4** and **6** exhibiting strong inhibition, possibly through ROS generation or DNA intercalation. Quinone derivatives (**10** and **12**) displayed dose-dependent cytotoxicity, suggesting redox-mediated apoptosis, while steroidal ganodermaside D (**20**) showed moderate and potent effects against hormone-related cancers (MCF-7 and PC-3), potentially *via* steroid receptor modulation. However, inconsistencies in MCF-7 inhibition between studies indicate that cell line-specific metabolic differences or compound stability may influence activity. Further mechanistic investigations, including transcriptomic profiling, ROS detection assays, and *in vivo* tumour models, are needed to validate these hypotheses. Quantum structure–activity relationship (QSAR) analyses could also guide the rational design of more selective derivatives.

# 3. Experimental

## 3.1. General experimental procedures

For large-scale fermentation, the fungus was grown on 4 mm petri dishes containing Yeast-Mold-Agar (YMA) and fermented using a solid rice medium, locally known as "tota chawal" (broken rice) in Karachi. For column chromatography, silica gel 60 (230–400 mesh, Merck, Germany) was used. Semi-pure compounds were further purified using a recycling preparative HPLC-LC-908 system (Japan) with a JAIGEL-ODS-M-80 column (250 mm × 20 mm, 4 μm, 80 Å). The eluent for reverse-phase chromatography was a 50% MeCN–50% $H_2O$ mixture. For normal-phase chromatography, a JAIGEL-SIL D-60–10 column was used.

The purity of isolated compounds was assessed using Merck TLC plates (silica gel 60 F254). A JASCO P-2000 polarimeter was used to measure optical rotations. UV spectra were recorded on a Hitachi U-3200 spectrophotometer, and IR spectra were obtained on a Bruker Alpha Platinum-ATR spectrometer using the ATR technique (4000–400 $cm^{-1}$, 4 $cm^{-1}$ resolution, 16 scans). Electron ionization mass spectra (EI-MS) were acquired using a JEOL JMS600H-1 mass spectrometer. NMR experiments were performed on Bruker Ascend 500, 600, and 800 MHz spectrometers in deuterated solvents, with chemical shifts referenced to TMS at 0.00 ppm for both $^1H$ and $^{13}C$ NMR. Coupling constants were reported in hertz (Hz).

## 3.2. Fungal material

Fresh horse dung was collected at Ecopark in Ahala, Yaoundé, Cameroon. Fungal isolation was carried out using the moist chamber protocol[49] with slight modifications. Briefly,

approximately 0.5 g of faeces was placed in four petri dishes containing filter paper. The petri dishes were pre-treated with a chloramphenicol solution (0.5 μM) to prevent bacterial growth. After 4 days of incubation, the first series of spores were observed, with subsequent series appearing after 8 and 15 days. The first series of spores was transferred to Malt Extract Agar (MEA) for further purification, resulting in the isolation of seven fungal strains, which were subjected to chemical pre-screenings. One of these strains showed potential for large-scale fermentation and was identified as *Fusarium solani* by Inqaba Biotec (https://inqababiotec.co.za/), through ITS nrDNA sequencing (Table S1†). A voucher specimen of the selected strain was stored at −80 °C in our laboratory under the number CECA065.

For identification, genomic DNA was extracted using the Quick-DNA™ Fungal/Bacterial kit (Zymo Research, Catalogue No. D6005). The ITS target region was amplified with OneTaq® Quick-Load® 2X Master Mix (NEB, Catalogue No. M0486) using ITS-1 and ITS-4 primers. The PCR product was analysed by gel electrophoresis and cleaned up enzymatically using the EXOSAP method. The extracted fragments were sequenced in both the forward and reverse directions (Nimagen, BrilliantDye™ Terminator Cycle Sequencing Kit V3.1, BRD3-100/1000) and subsequently purified (Zymo Research, ZR-96 DNA Sequencing Clean-up Kit™, Catalogue No. D4050). The purified fragments were analysed on the ABI 3500xl Genetic Analyser (Applied Biosystems, ThermoFisher Scientific). The resulting sequence data (*.ab1 files) were processed using DNASTAR software and identified through a BLAST search (NCBI).

### 3.3. Fermentation and extraction

Ten 500 mL-Erlenmeyer flasks, each containing 80 g of broken rice (tota chawal) and 100 mL distilled water, were autoclaved and inoculated with well-grown *Fusarium solani* cultures from Yeast-Mold-Agar (YMA) plates. The flasks were incubated at 20 °C in an air-conditioned room. After 15 days, the cultures were harvested, and the fungal mycelia were extracted with ethyl acetate. The filtrate was concentrated under reduced pressure, yielding 4.2 g of purple crude extract.

### 3.4. Isolation

The organic extract (4 g) was subjected to silica gel column chromatography and eluted with mixtures of *n*-hexane/acetone (0–100% acetone, v/v) of increasing polarity, followed by acetone/methanol (9 : 1 to 8 : 2, v/v), resulting in 100 fractions ($fr_1$–$fr_{100}$, ∼400 mL each). Fractions $fr_{51}$–$fr_{54}$ formed a precipitate, which was washed with *n*-Hex/acetone (95 : 5, v/v) to yield compound **5** (15 mg, yellow amorphous powder, $t_R$: 22 min). Based on TLC profiles, the fractions were grouped into 7 main series (I–VII). Series I (200 mg) and VII (1.2 g), eluted with pure *n*-hexane and 10–20% methanol in acetone (v/v), were complex mixtures and were not further investigated.

Series II (20 mg), obtained with 5% acetone in hexane, was further purified by normal-phase preparative HPLC equipped with a JAIGEL-SIL (D-60-10) column, using a mixture of 1% methanol in chloroform ($CHCl_3$) as the eluent. This purification yielded compound **8** (15 mg), a pigment with an intense purple colour ($t_R$: 22 min). Series III (37 mg), obtained with *n*-Hex/acetone (90 : 10, v/v), was purified by normal-phase preparative HPLC, using 1% methanol in chloroform as the eluent, to afford compound **9** (5.2 mg), an orange pigment ($t_R$: 18 min).

Series IV (1.2 g), obtained with *n*-Hex/acetone (80 : 20, v/v), was separated by silica gel column chromatography using a $CHCl_3$/MeOH (99 : 1, v/v) mixture, resulting in compounds **16** (7.2 mg, white gum, $t_R$: 12 min), **6** (105 mg, yellow needle crystals, $t_R$: 18 min), and sub-fractions $IV_A$ and $IV_B$. Sub-fraction $IV_A$ (8.3 mg) was further purified on a Sephadex LH-20 column using 50% MeOH in $CH_2Cl_2$, yielding compound **20** (4 mg, yellow oil). Sub-fraction $IV_B$ (88 mg) was purified by reverse phase preparative HPLC using 50% MeCN in $H_2O$, yielding two pink pigments: compounds **12** (3.8 mg, $t_R$: 32 min) and **11** (9.2 mg, $t_R$: 36 min).

Series V (300 mg), eluted from the main column with *n*-Hex/acetone (70 : 30, v/v) was further subjected to column chromatography over silica gel using a $CH_2Cl_2$/MeOH (96 : 4, v/v) mixture to give sub-fractions $V_A$–$V_C$. Sub-fraction $V_A$ (45 mg) was purified by reverse phase preparative HPLC (50% MeCN–50% $H_2O$), to afford compounds **3** (3.1 mg, yellow pigment, $t_R$: 18 min), and **1** (1.3 mg, yellow pigment, $t_R$: 22 min). Using the same HPLC method and equipment, sub-fraction $V_B$ (12 mg) yielded compounds **7** (0.5 mg, white amorphous powder, $t_R$: 25 min) and **2** (1.1 mg, yellow pigment, $t_R$: 28 min). Lastly, sub-fraction $V_C$ (30 mg) afforded compounds **19** (6 mg, white gum, $t_R$: 30 min), and **18** (10 mg, white gum, $t_R$: 36 min).

Series VI (102 mg), which was previously eluted from the main column with *n*-Hex/acetone (60 : 40, v/v) was further subjected to silica gel column chromatography using an isocratic mixture of $CH_2Cl_2$/acetone (85 : 15, v/v) to afford compounds **21** (7.2 mg, white neat solid), and sub-fractions $VI_A$ and $VI_B$. Both sub-fractions were separately purified by reverse preparative HPLC using MeCN/$H_2O$ (1 : 1, v/v). Sub-fractions $VI_A$ provided orange pigments of **10** (1.5 mg, $t_R$: 30 min), and **17** (1.3 mg, $t_R$: 32 min). Sub-fractions $VI_B$ yielded orange pigments, including **15** (2.3 mg, $t_R$: 28 min), **14** (4.3 mg, $t_R$: 34 min), and **13** (5.2 mg, $t_R$: 38 min).

### 3.5. Physico-chemical properties of compounds 1–4

Fusaphenazinone (**1**): yellowish pigment; $[\alpha]_D25$ 0 (*c* 0.10, $CHCl_3$); UV ($CHCl_3$) $\lambda_{max}$ (Abs.) 256 (1.55), 267 (1.52), 371 (1.70) nm; IR (ATR) $\nu_{max}$ 2923, 2852, 1769, 1557, 1525, 1305, 1188, 1158, 957, 901, 759, 671 $cm^{-1}$; $^1H$ and $^{13}C$ NMR data, Table 1; EI-MS *m*/*z* (rel. int., %): 280 (11), 265 (26), 249 (32), 235 (6), 220 (13), 205 (6), 193 (9), 179 (5), 149 (8), 111 (4), 85 (5), 71 (9), 57 (12), 44 (100); HREI-MS *m*/*z* 280.0846 $[M]^{\bullet+}$ (mol. formula $C_{16}H_{12}N_2O_3$, calcd value 280.0848).

4-Methylphenazine-1-carboxylic acid (**2**): yellowish pigment; UV ($CHCl_3$) $\lambda_{max}$ (Abs.) 257 (1.51), 266 (1.50), 372 (2.09) nm; IR (ATR) $\nu_{max}$ 2922, 2852, 1715, 1569, 1531, 1464, 1264, 1293, 800, 760, 741 $cm^{-1}$; $^1H$ and $^{13}C$ NMR data, Table 1; EI-MS *m*/*z* (rel. int., %): 238 (0.8), 194 (100), 193 (32.7), 102 (2.6), 179 (1.1), 128 (0.6); HREI-MS *m*/*z* 238.0744 $[M]^{\bullet+}$ (mol. formula $C_{14}H_{10}N_2O_2$, calcd value 238.0742).

1-Acetyl-4-hydroxyphenazine (**3**): yellowish pigment; UV ($CHCl_3$) $\lambda_{max}$ (Abs.) 247 (2.14), 264 (1.99), 368 (1.38) nm; IR (ATR) $\nu_{max}$ 3400, 2929, 2851, 1684, 1590, 1398, 1364, 1246, 667, 494 $cm^{-1}$; $^1H$ and $^{13}C$ NMR data, Table 1; EI-MS *m*/*z* (rel. int., %): 238 (13), 221 (60), 195 (100), 178 (42), 162 (29), 145 (12), 119 (35), 102 (29); HREI-MS *m*/*z* 238.0740 $[M]^{\bullet+}$ (mol. formula $C_{14}H_{10}N_2O_2$, calcd value 238.0742).

9,10-dimethylphenoxazine-4-carboxylic acid (**4**): yellowish pigment; UV ($CHCl_3$) $\lambda_{max}$ (Abs.) 262 (0.50), 374 (0.13) nm; IR (ATR) $\nu_{max}$ 3366, 2923, 2853, 1737, 1575, 1540, 1464, 1416, 1377, 1174, 1113, 768 $cm^{-1}$; $^1H$ and $^{13}C$ NMR data, Table 1; EI-MS *m*/*z* (rel. int., %): 255 (8), 210 (100), 180 (55), 150 (8), 120 (21), 105 (6), 90 (12); HREI-MS *m*/*z* 255.0893 $[M]^{\bullet+}$ (mol. formula $C_{15}H_{13}NO_3$, calcd value 255.0895).

### 3.6. Biological assays

**3.6.1 Antibacterial and biofilm formation inhibition assays.** The antibacterial activity of selected isolated compounds was assessed against two *Staphylococcus aureus* strains, including a MRSA strain (NCTC 13277) and a biofilm-forming strain (ATCC 6538), as well as *Escherichia coli* (ATCC 25922) using the Mueller-Hinton broth (MHB) microdilution method, as previously described by Maharjan *et al.* (2022).[50] Stock solutions of the tested compounds (20 mM) were prepared in DMSO and two-fold diluted in MHB broth, ranging from 400 to 3.125 μM (final DMSO concentrations: 2% to 0.0625%, solvent controls confirmed no growth inhibition). The minimum inhibitory concentration (MIC) was defined as the lowest concentration of the test compounds that did not support visible growth.

**3.6.2 Antifungal assay.** *Candida albicans* (ATCC 36082) was cultured on Sabouraud Dextrose Agar (SDA) and transferred to Sabouraud Dextrose Broth (SDB) for overnight incubation at 37 °C with shaking. A broth microdilution assay was then performed to assess the antifungal effects of the isolated compounds, which were serially diluted two-fold in SDB. A total of 100 μL of each dilution was added to a 96-well plate, followed by 100 μL of a 1000-fold diluted overnight culture ($OD_{600} = 1$) in SDB, resulting in a final inoculum concentration of 2–4 × $10^5$ CFU $mL^{-1}$. Plates were incubated at 37 °C for 24 hours, and the MIC values were determined.

**3.6.3 Cytotoxicity assay.** The MCF-7 (breast), HeLa (cervical), and PC-3 (prostate) cancer cell lines were purchased from ATCC (USA) and stored in the cell culture bank of the Dr Panjwani Centre for Molecular Medicine and Drug Research (ICCBS, University of Karachi, Pakistan). The cells were cultured in DMEM supplemented with 10% foetal bovine serum (FBS; Gibco) at 37 °C in a 5% $CO_2$ humidified atmosphere. For cytotoxicity assessment, cells were seeded at 6000 cells/well and treated with varying concentrations (6.25 μM, 12.5 μM, 25 μM, 50 μM, and 100 μM) of each test compound for 24–72 hours. Untreated cells served as the negative control, while 0.5% DMSO-treated cells were used as the solvent control. Doxorubicin was included as the positive control. The final DMSO concentration did not exceed 0.5% (v/v) in any treatment. Cytotoxicity was evaluated using the MTT assay. After treatment, 20 μL of MTT solution (5 mg $mL^{-1}$ in phosphate-buffered saline) was added to each well and incubated for 4 hours at 37 °C (5% $CO_2$). The resulting formazan crystals were solubilized, and absorbance was measured at 540 nm using a Multiskan™ GO microplate reader (Thermo Scientific, USA). For each compound, the percent inhibition was calculated, and the half-maximal inhibitory concentration ($IC_{50}$), defined as the concentration required for 50% inhibition of cell growth relative to untreated controls, was determined by nonlinear regression analysis of dose–response data as previously described by Maharjan *et al.* (2022).[50] Dose-dependent inhibition curves are provided in ESI (Fig. S34–S36).†

## 4. Conclusions

This study reports the isolation of four new phenazine-derived pigments and seventeen known compounds from *Fusarium solani*, along with an evaluation of their antimicrobial and cytotoxic activities. None of the compounds exhibited significant antimicrobial effects against *Staphylococcus aureus*, *Candida albicans*, and *Escherichia coli*, although compounds **5** and **11** showed weak to moderate activity against *C. albicans* and *S. aureus*. In contrast, the new compound, 9,10-dimethylphenoxazine-4-carboxylic acid (**4**), showed strong cytotoxicity against MCF-7 human breast cancer cell lines. Some known quinone-derived compounds, including **10**, **12**, and **13**, exhibited potent activity against the tested cancer cell lines. These findings suggest that the primary bioactivity of phenazine- and quinone-derived pigments is cytotoxic, highlighting their strong potential for anticancer drug development. However, our findings regarding the potencies of quinones **8** and **12** on MCF-7 breast cancer cells differ from those reported by Trisuwan and collaborators (2010).[21] Further research, including structure–activity relationship (SAR) studies, is necessary to optimise these compounds and the new derivative **4** for enhanced chemotherapeutic efficacy.

## Data availability

The data generated and analysed during this study are available from the corresponding author upon reasonable request. Data related to the chemical structures and spectroscopic analysis of the isolated compounds are available in the ESI.†

## Author contributions

B. Y. G. M., P. D., and J. T.: isolation, identification, and cultivation of the fungus. B. Y. G. M.: methodology, large scale fermentation, purification and isolation of compounds, spectroscopic analysis, and data curation. B. Y. G. M. and R. M.: bioassays, data curation, and preparing the original draft manuscript. B. Y. G. M., I. L. M., and S. F. K.: structure elucidation. G. L. M. T., M. I. C., and S. F. K.: reviewing, editing, and correcting the draft. B. Y. G. M., J. T., G. L. M. T., and S. F. K.: conceptualization. M. I. C. and S. F. K.: supervision, funding acquisition. All authors have read and agreed to the published version of the manuscript.

## Conflicts of interest

The authors declare no conflict of interest.

## Acknowledgements

B. Y. G. M. gratefully acknowledges The World Academy of Sciences (TWAS) for an eight-month Postdoctoral Fellowship (FR number: 3240325064) under the ICCBS-UNESCO-TWAS programme, which supported his research visit to the H.E.J. Research Institute of Chemistry, ICCBS, University of Karachi, Pakistan. He also expresses his gratitude to the Ministerial Standing Committee on Scientific and Technological Cooperation (COMSTECH) of the Organization of Islamic Cooperation (OIC) for partially supporting his living expenses at the ICCBS. This work was conducted as part of the Humboldt Research Hub-CECANAPROF (3.4-CMR-Hub) on antimicrobial natural products from fungi (**https://cecanaprof.com/**), funded by the Alexander von Humboldt Foundation. The authors further acknowledge the German Academic Exchange Service (DAAD) for providing equipment grants (PKZ 308665 - Ref. ST 42) to their laboratory at the Higher Teacher Training College, University of Yaoundé I, Cameroon.

## References

1 A. A. Farouq, D. K. Abdullah, F. Hooi-Ling, N. Abdullah, S. S. Malaysia and J. Biol, *J. Agric. Saf. Health.*, 2012, **2**, 44–51.
2 A. Mumpuni, A. Amurwanto and D. J. Wahyono, *Biodivers. J.*, 2021, **22**, 1550–1557.
3 A. S. Jasim, B. A. Abass and I. M. Al-Rubayae, *Arch. Razi. Inst.*, 2021, **76**, 1333–1341.
4 M. J. Richardson, *Mycol. Res.*, 2001, **105**, 387–402.
5 M. A. Moghalles and S. M. Al-Bader, *YJAVS*, 2014, **1**, 22–26.
6 V. Edel-Hermann and C. Lecomte, *Phyopathology*, 2019, **109**, 512–530.
7 R. Poorniammal, S. Prabhu, L. Dufossé and J. Kannan, *J. Fungi*, 2021, **7**, 692.
8 S. R. M. Ibrahim, A. Sirwi, B. G. Eid, S. G. A. Mohamed and G. A. Mohamed, *J. Fungi*, 2021, **7**, 943.
9 B. S. Menezes, L. S. Solidade, A. A. Conceição, M. N. Santos Junior, P. L. Leal, E. S. de Brito, K. M. Canuto, S. Mendonça, F. G. de Siqueira and L. M. Marques, *Appl. Microbiol. Biotechnol.*, 2020, **10**, 117.
10 S. Sarrocco, *Pest. Manag. Sci.*, 2016, **72**, 643–652.
11 M. Vašutová, P. Mleczko, A. López-García, I. Macek, G. Boros, J. Ševcík, S. Fujii, D. Hackenberger, I. H. Tuf, E. Hornung, B. Páll-Gergely and R. Kjøller, *Mycorrhiza*, 2019, **29**, 413–434.
12 B. Y. G. Mountessou, M. E. G. Anoumedem, B. M. Kemkuignou, Y. Marin-Felix, F. Surup, M. Stadler and F. S. Kouam, *Beilstein J. Org. Chem.*, 2023, **19**, 1555–1561.
13 M. E. G. Anoumedem, B. Y. G. Mountessou, F. S. Kouam, A. Narmani and F. Surup, *Antibiotics*, 2020, **9**, 753.
14 M. G. Happi, S. F. Kouam, F. M. Talontsi, C. Nkenfou, F. Longo, B. T. Ngadjui and M. Spiteller, *Z. Naturforsch.*, 2013, **70**, 625–630.
15 V. Shanmugaiah, N. Mathivanan and B. Varghese, *J. Appl. Microbiol.*, 2010, **108**, 703–711.
16 J. A. VanAllan, G. A. Reynolds and R. E. Adel, *J. Org. Chem.*, 1962, **27**, 1659–1664.
17 G. W. Rewcastle, W. A. Denny and B. C. Baguley, *J. Med. Chem.*, 1987, **30**, 843–851.
18 A. Cimmino, Z. Bahmani, S. Castaldi, M. Masi, R. Isticato, J. Abdollahzadeh, J. Amini and A. Evidente, *J. Agric. Food Chem.*, 2021, **69**, 12143–12147.
19 G. P. Jones, D. G. Lewis and M. E. Tate, *Acta Cryst.*, 1988, **C44**, 2220–2222.
20 K. Ströch, A. Zeeck, N. Antal and H. P. Fiedler, *J. Antibiot.*, 2005, **58**, 103–110.
21 K. Trisuwan, N. Khamthong, V. Rukachaisirikul, S. Phongpaichit, S. Preedanon and J. Sakayaroj, *J. Nat. Prod.*, 2010, **73**, 1507–1511.
22 I. Kurobane, L. C. Vining, A. G. McInnes and J. A. Walter, *Can. J. Chem.*, 1980, **58**, 1380–1385.
23 J. H. Tatum and R. A. Baker, *Phytochemistry*, 1983, **22**, 543–547.
24 Y. Wen, Y. Lv, J. Hao, H. Chen, Y. Huang, C. Liu, H. Huang, Y. Ma and X. Yang, *Nat. Prod. Res.*, 2020, **34**, 1879–1883.
25 T. Kurobane, L. C. Vining, A. G. McInnes and D. G. Smith, *Can. J. Chem.*, 1978, **56**, 1593.
26 N. Khan, F. Afroz, M. N. Begum, S. R. Rony, S. Sharmin, F. Moni, C. M. Hasan, K. Shaha and M. H. Sohrab, *Toxicol Rep*, 2018, **5**, 970–976.
27 D. Bergeron, B. Caron and P. Brassard, *J. Org. Chem.*, 1993, **58**, 509–511.
28 J. H. Tatum, R. A. Baker and R. E. Berr, *Phytochemistry*, 1985, **24**, 3019–3021.
29 D.-L. Zhao, D. Wang, X.-Y. Tian, F. Cao, Y.-Q. Li and C.-S. Zhang, *Mar. Drugs*, 2018, **16**, 36.
30 P. Wang, Y. Cui, C. Cai, H. Chen, Y. Dai, P. Chen, F. Kong, J. Yuan, X. Song and W. Mei, *Mar. Drugs*, 2018, **17**, 4.
31 H. Liu, C. Yan, C. Li, T. You and Z. She, *Molecules*, 2020, **25**, 576.
32 S.-J. Wang, H.-W. Liu, Y.-Q. Wang, L. Bao, X.-L. Yang and H.-A. Wen, *Mycosystema*, 2013, **32**, 1028–1033.
33 H. Finnemore, *J. Chem. Soc.*, 1908, **93**, 1513–1519.
34 S. P. Diggle, S. Matthijs, V. J. Wright, M. P. Fletcher, S. R. Chhabra, I. L. Lamont, X. Kong, R. C. Hider, P. Cornelis, M. Cámara and P. Williams, *Chem. Biol.*, 2007, **14**, 87–96.
35 D. Li, N. Oku, A. Hasnada, M. Shimizu and Y. Igarashi, *Beilstein J. Org. Chem.*, 2018, **14**, 1446–1451.
36 D. Staerk, J. R. Kesting, M. Sairafianpour, M. Witt, J. Asili, S. A. Emami and J. W. Jaroszewski, *Phytochemistry*, 2009, **70**, 1055–1061.
37 Y. Weng, J. Lu, L. Xiang, A. Matsuura, Y. Zhang, Q. Huang and J. Qi, *Biosci., Biotechnol., Biochem.*, 2011, **75**, 800–803.
38 Q.-X. Wang, S.-F. Li, F. Zhao, H.-Q. Dai, L. Bao, R. Ding, H. Gao, L.-X. Zhang, H.-A. Wen and H.-W. Liu, *Fitoterapia*, 2011, **82**, 777–781.
39 H. Kawagishi, R. Katsumi, T. Sazawa, T. Mizuno, T. Hagiwara and T. Nakamura, *Phytochemistry*, 1988, **21**, 2111–2119.

40 S. Kumaria, V. Khanna and N. Sharma, *Int. J. Pest Manag.*, 2024, **70**, 1086–1099.
41 A. Upadhyay and S. Srivastava, *Microbiol. Res.*, 2011, **166**, 323–335.
42 A. H. Mussa, A. F. Abdulkareem, H. F. Abbas and H. Farhan, *Syst. Rev. Pharm.*, 2020, **11**, 408.
43 V. F. Cardozo, A. G. Oliveira, E. K. Nishio, M. R. E. Perugini, C. G. T. J. Andrade, W. D. Silveira, N. Durán, G. Andrade, R. K. T. Kobayashi and G. Nakazato, *Ann. Clin. Microbiol. Antimicrob.*, 2013, **12**, 1–8.
44 O. P. Martínez-Rodríguez, R. García-Contreras, R. Aguayo-Ortiz and M. Figueroa, *Biofouling*, 2023, **39**, 830–837.
45 H. Satriawan, T. C. Teoh, M. Rizman-Idid, A. Krishnan, N. A. Bakar and S. A. Alias, *Chiang Mai J. Sci.*, 2024, **51**, e2024043.
46 D. K. Morales, N. J. Jacobs, S. Rajamani, M. Krishnamurthy, J. R. Cubillos-Ruiz and D. A. Hogan, *Mol. Microbiol.*, 2010, **78**, 1379–1392.
47 W. Xun, B. Gong, X. Liu, X. Yang, X. Zhou and L. Jin, *Int. J. Mol. Sci.*, 2023, **24**, 11274.
48 R. J. N. Frandsen, S. A. Rasmussen, P. B. Knudsen, S. Uhlig, D. Petersen, E. Lysøe, C. H. Gotfredsen, H. Giese and T. O. Larsen, *Sci. Rep.*, 2016, **6**, 26206.
49 D. L. Hawksworth, *Mycologist's Handbook*, Commonwealth Mycological Institute, Kew, Hawksworth, UK, 1974.
50 R. Maharjan, A. I. Khan, M. Nadeem-ul-Haque, M. Maresca, M. I. Choudhary, F. Shaheen and S. U. Simjee, *Probiotics. Antimicrob. Proteins*, 2022, **14**, 391–405.